Magnetic properties in monolayers of a model polydisperse ferrofluid

Tamás Kristóf
Department of Physical Chemistry, University of Veszprém, H-8201 Veszprém, P.O. Box 158, Hungary

István Szalai
Department of Physics, University of Veszprém, H-8201 Veszprém, P.O. Box 158, Hungary
(Received 25 June 2005; published 25 October 2005)

The influence of polydispersity on the equilibrium properties of monolayers of three-dimensional dipolar spheres with short-range repulsive interactions is studied by means of Monte Carlo simulations and a high field approximation perturbation theory. The particle distribution in the simulations is realized in the semigrand ensemble by tuning appropriately the underlying particle distribution density. The magnetization curves are calculated as functions of density and temperature, and the obtained results are compared with the data determined in a monodisperse equivalent of the system. In-plane and out-of-plane initial magnetic susceptibilities are determined using external fields applied parallel or normal to the monolayer plane. Susceptibility data for the true two- and three-dimensional counterparts of the system are also calculated for comparison. Our findings for the magnetic properties can partly be explained by the structural characteristics obtained from the simulations.

DOI: 10.1103/PhysRevE.72.041105 PACS number(s): 05.20.Jj, 61.20.Ja, 75.50.Mm, 75.70.Ak

I. INTRODUCTION

Monolayers of dipolar particles have recently attracted considerable attention [1–6]. This is partly motivated by the current technological interest in thin-film devices and by the need to understand many experimental situations such as adsorption of amphiphilic molecules at an air/water interface, magnetic microspheres floating on a liquid surface, or thin ferrofluid films under the influence of external fields. In confined systems the orientational entropy of the system is generally restricted, and thus new properties without any bulk analog may emerge. In quasi-two-dimensional (q2D) ferrofluids, e.g., an external magnetic field perpendicular to the surface (or confinement walls) can be used to induce tunable repulsive interactions between the particles.

Recently, Weis and co-workers [2–4,6] have used simulations and theory to investigate the structures formed in q2D systems of strongly interacting dipolar spheres in the absence or in the presence of the external field. Duncan and Camp [5] examined the dynamics of the self-assembly of dipolar soft spheres in monolayers. However, the thermodynamic and magnetization properties of such q2D model systems have been studied less extensively: besides the work of Lomba *et al.* [2], we are only aware of the work of Gao *et al.* [7] who simulated the fluid-fluid equilibria of dipolar Lennard-Jones (Stockmayer) model systems.

Ferrofluids (magnetic fluids) are stable colloidal dispersions of nanometric magnetic particles coated with ionic groups or polymer surfactants in liquid carriers, which have a wide range of technological applications [8]. The constituent nanoparticles are roughly spherical and their permanent magnetic dipole moments are proportional to their volumes. Therefore the key interaction in ferrofluids is the long-range dipole-dipole potential besides the obvious spherical repulsion between the magnetic cores, and the short-range interactions due to the coatings (van der Waals attractions and electrostatic or steric repulsions) are less important [9].

The characteristic feature of real ferrofluids is that the nanoparticles differ in size and magnetic moment. This polydispersity affects the equation of state of the system and may have an important consequence for the phase behavior, in particular for the fluid-fluid coexistence [10,11]. Polydispersity also affects the equilibrium magnetization of these fluids: recently, the influence of realistic polydispersity on the equilibrium magnetization properties of model ferrofluids was investigated, and it was found that the magnetization is greater in the polydisperse system than in its monodisperse equivalent [12].

Simulations of polydisperse systems are generally performed with a discretization of the particle distribution [12,13], reducing the number of components to a small value and thus bringing about some errors, due to finite-size effects, in the results of the calculations. Utilizing the semigrand ensemble Monte Carlo approach [14,15] that incorporates resizing moves of the particles, quasicontinuous particle distributions can be realized. Although this technique was originally restricted to systems with variable polydispersity, i.e., to systems where the form of the particle distribution also depends on the thermodynamic conditions [16], it is possible to determine the form of the underlying (sampling) distribution for the resizing moves during the simulation, for which the ensemble averaged particle distribution fits the particle distribution to be generated in the system [17]. There are also related approaches [18–20] based on Monte Carlo simulations in the grand canonical ensemble, the latter [20] involves employing a self-consistent iterative determination of the chemical potential distribution (conjugate to the composition distribution). This is a more sophisticated technique; nevertheless, it has a drawback in view of the present study since the overall number density of the system cannot be kept fixed.

In this paper, we study the influence of polydispersity on the magnetic properties of model ferrofluid monolayers by means of simulation and theory. In the simulations, the pre-

scribed particle distribution is realized as a quasicontinuous particle distribution. Magnetization curves and initial susceptibilities are calculated and the microstructures are analyzed as functions of density and temperature, and the obtained results are compared with the data determined in the monodisperse and in the true two- and three-dimensional (2D and 3D) counterparts of the systems. Since there is a sizable body of thermodynamic perturbation theoretical research available, which is devoted to the study of bulk properties of magnetic [9,10,21,22] or the corresponding dipolar molecular fluids [23–25], here we use again, continuing our perturbation theoretical study [12], a first order cluster expansion theory to predict the magnetization curves in q2D and initial susceptibilities in all studied dimensions.

II. METHOD

A. Model

The system consists of spherical particles of diameter σ_i, which have permanent point dipole (magnetic) moments m_i. The short-range repulsive interaction between particles i and j are modeled by a shifted and truncated Lennard-Jones pair potential [26]:

$$\varphi_{ij,r}^{(D)} = 4\varepsilon\left[\left(\frac{\sigma_{ij}}{r_{ij}}\right)^{12} - \left(\frac{\sigma_{ij}}{r_{ij}}\right)^{6} - \left(\frac{\sigma_{ij}}{r_c}\right)^{12} + \left(\frac{\sigma_{ij}}{r_c}\right)^{6}\right],$$

$$r_{ij} \leqslant r_c = \sigma_{ij} 2^{1/6}, \tag{1}$$

where ε is the energy parameter, r_{ij} is the interparticle distance, $\sigma_{ij}=(\sigma_i+\sigma_j)/2$, and r_c is the cutoff radius ($D=3\mathrm{D},\mathrm{q2D},2\mathrm{D}$). This form of nearly hard sphere repulsion takes into account the fact that the particle size in ferrofluids exceeds the magnetic core diameter σ_i.

The three-dimensional dipole-dipole potential between particles i and j is given by

$$\varphi_{ij,d}^{(D)} = \frac{\mathbf{m}_i \cdot \mathbf{m}_j}{r_{ij}^3} - 3\frac{(\mathbf{m}_i \cdot \mathbf{r}_{ij})(\mathbf{m}_j \cdot \mathbf{r}_{ij})}{r_{ij}^5}, \quad D = 3\mathrm{D},\mathrm{q2D}. \tag{2}$$

In the q2D case the spheres and the centers of the dipole moments are constrained to lie on the same plane while the dipole vectors can freely rotate in 3D. Here, the dipole-dipole pair potentials are quoted in Gaussian units to facilitate the comparison of the 2D and 3D results.

In true 2D the dipole vectors allow one to rotate only in the plane of the dipole centers and the dipole-dipole potential can be written as

$$\varphi_{ij,d}^{(2\mathrm{D})} = \frac{\mathbf{m}_i \cdot \mathbf{m}_j}{r_{ij}^2} - 2\frac{(\mathbf{m}_i \cdot \mathbf{r}_{ij})(\mathbf{m}_j \cdot \mathbf{r}_{ij})}{r_{ij}^4}. \tag{3}$$

This interaction potential is derived on the basis of the two-dimensional Laplace equation via the application of the multipole potential expansion [27]. It is long ranged in 2D as well as Eq. (2) in 3D. It is easy to see that the orientation part of Eq. (3) can be expressed by a single cosine function of the orientation of dipole vectors and the interparticle radius vector [27] and therefore its mathematical shape makes easier the analytical calculations in 2D.

The interaction of dipole moments with an external magnetic field $\mathbf{H}$ in all dimensions is

$$\varphi_i^{ext} = -\mathbf{m}_i \cdot \mathbf{H}. \tag{4}$$

The particle polydispersity is described by the gamma distribution [28],

$$p(x) = \frac{x^{\Theta}}{x_0}\left(\frac{x}{x_0}\right)^{a}\frac{\exp(-x/x_0)}{\Gamma(a+1)}, \tag{5}$$

where x is the magnetic core diameter of particles, x_0 and a are the parameters of the distribution, Γ denotes the gamma function, and $x^{\Theta}=1$ nm is taken as the unit length [to render $p(x)$ dimensionless]. For spherical particles, $\sigma=x$, and the magnetic moment reads

$$m(x) = M_d\frac{\pi}{6}x^3, \tag{6}$$

where M_d represents the bulk magnetization of the ferromagnetic component.

B. Theory

Our calculation is based on the high field perturbation approximation originally introduced by Buyevich and Ivanov [21]. In the framework of this theory we assume that the orientation of magnetic dipoles is governed mainly by the external field and the dipole-dipole interaction can be considered as a perturbation. According to this assumption the total pair potential of the D dimensional reference system is

$$\varphi_0^{(D)} = \sum_{i<j}\varphi_{ij,r}^{(D)} + \sum_i \varphi_i^{ext}, \quad D = 3\mathrm{D},\mathrm{q2D},2\mathrm{D}. \tag{7}$$

Therefore the pair correlation function of the reference system reads

$$g_{ij,0}^{(D)}(r_{12},\omega_1,\omega_2) = f_i^{(D)}(\omega_1)g_{ij,r}^{(D)}(r_{12})f_j^{(D)}(\omega_2),$$

$$D = 3\mathrm{D},\mathrm{q2D},2\mathrm{D}. \tag{8}$$

In this paper, the mean-field approximation is used for the pair correlation functions of the shifted and truncated Lennard-Jones fluids:

$$g_{ij,r}^{(D)}(r_{12}) = \begin{cases} 1, & \text{if } r_{12} \geqslant \sigma_{ij} \\ 0, & \text{if } r_{12} < \sigma_{ij} \end{cases}, \quad D = 3\mathrm{D},\mathrm{q2D},2\mathrm{D}. \tag{9}$$

The single particle orientation distribution function for the different dimensions is

$$f_i^{(D)}(\omega_1) = \exp(\alpha_i \cos\vartheta_i)\begin{cases} \alpha_i \sinh^{-1}(\alpha_i), & \text{if } D = 3\mathrm{D},\mathrm{q2D} \\ [I_0(\alpha_i)]^{-1}, & \text{if } D = 2\mathrm{D} \end{cases}, \tag{10}$$

where $\alpha_i=m_iH/kT$ with k and T being the Boltzmann constant and the temperature, ϑ_i is the angle between the ith dipole and the external field, and $I_0(\alpha)$ is the modified Bessel function of the first kind of zero order. The corresponding configurational integral of the reference system can be written as

$$Q_0^{(D)} = Q_r^{(D)} \begin{cases} \prod_i (\alpha_i)^{-1} \sinh(\alpha_i), & \text{if } D = 3\text{D,q2D} \\ \prod_i I_0(\alpha_i), & \text{if } D = 2\text{D}. \end{cases} \tag{11}$$

In our approximation, the knowledge of the configurational integral $Q_r^{(D)}$ is not necessary to the calculation of the magnetic properties; therefore we do not specify the corresponding formula. The long-ranged dipole-dipole interaction in Eqs. (2) and (3) is considered as a perturbation and, on the basis of an expansion of the total configurational integral ($Q^{(D)}$) with respect to the Mayer function, we obtain:

$$\ln \frac{Q^{(D)}}{Q_0^{(D)}} \cong \frac{1}{2V} \sum_{i,j} N_i N_j \int d^{(D)}\mathbf{r_1} d^{(D)}\mathbf{r_2} d^{(D)}\omega_1 d^{(D)}\omega_2 \times f_i^{(D)}(\omega_1) f_{\mathrm{M},ij}^{(D)}(\mathbf{r_{12}}, \omega_1, \omega_2) f_j^{(D)}(\omega_2),$$

$$D = 3\text{D,q2D,2D}, \tag{12}$$

where V is the volume (area) of the system, $f_{\mathrm{M},ij}^{(D)}$ represents the Mayer function, and N_i denotes the number of dipoles bearing dipole moment m_i. Furthermore, $d^{(3\mathrm{D})}\mathbf{r_1} = d^3 r_1$, $d^{(\mathrm{q2D})}\mathbf{r_1} = d^{(2\mathrm{D})}\mathbf{r_1} = d^2 r_1$, $d^{(3\mathrm{D})}\omega_1 = d^{(\mathrm{q2D})}\omega_1 = (4\pi)^{-1} \sin\vartheta_1 \, d\vartheta_1 d\phi_1$, and $d^{(2\mathrm{D})}\omega_1 = (2\pi)^{-1} d\vartheta_1 d\phi_1$, where ω_1 is the three- or two-dimensional solid angle. Here the Mayer function is defined in the usual way:

$$f_{\mathrm{M},ij}^{(D)}(\mathbf{r_{12}}, \omega_1, \omega_2) = \exp\left(- \frac{\varphi_{ij,d}^{(D)}(\mathbf{r_{12}}, \omega_1, \omega_2)}{kT} \right) - 1,$$

$$D = 3\text{D,q2D,2D}. \tag{13}$$

To perform the integration in Eq. (12), a further approximation is necessary: in 2D and q2D, we expand the Mayer function into first order Taylor series, however, in order to improve the approximation for the susceptibility for real 3D systems (see Ref. [12]), a third order Taylor series expansion is used in Eq. (13). In q2D, in contrast to 3D and 2D, besides the in-plane external field ($H_\parallel$) we can introduce an external field which is perpendicular to the surface ($H_\perp$). Naturally, the configurational integral [Eq. (12)] depends on this choice. The integration with respect to ω_1 and ω_2 can be performed analytically in all dimensions. In 3D and q2D the remaining integration with respect to $\mathbf{r_1}$ and $\mathbf{r_2}$ can also be carried out analytically on an infinitely long cylinder and an infinitely long rectangle to avoid the depolarization. As the two integrals appearing in q2D are not long-ranged, they can be calculated on 2D "spheres."

From the configurational integral the field dependent free energy can be obtained. According to the two external field orientations the q2D free energies are

$$F_\parallel^{(\mathrm{q2D})} = F_r^{(\mathrm{q2D})} - kT \sum_i N_i \ln \frac{\sinh(\alpha_i)}{\alpha_i} - \frac{\pi}{2V} \sum_{i,j} N_i N_j m_i m_j L(\alpha_i) L(\alpha_j), \tag{14}$$

and

$$F_\perp^{(\mathrm{q2D})} = F_r^{(\mathrm{q2D})} - kT \sum_i N_i \ln \frac{\sinh(\alpha_i)}{\alpha_i} + \frac{\pi}{V} \sum_{i,j} N_i N_j m_i m_j L(\alpha_i) L(\alpha_j), \tag{15}$$

where $L(\alpha) = \coth(\alpha) - 1/\alpha$ is the Langevin function. In this paper, we do not study the magnetization for 3D and true 2D systems therefore we present the corresponding free energies only with such kind of terms which contribute to the initial susceptibility. (The 3D and true 2D free energy functions are rather complicated and will be published in our future work [29].) The initial susceptibility is proportional to the second derivative of the field dependent free energy with respect to the field strength; in the following we give their power expansions in second order:

$$F^{(2\mathrm{D})} = F_r^{(2\mathrm{D})} - \frac{kT}{4} \sum_i N_i \alpha_i^2 - \frac{\pi}{8V} \sum_{i,j} N_i N_j m_i m_j \alpha_i \alpha_j + O(H^3), \tag{16}$$

and

$$F^{(3\mathrm{D})} = F_r^{(3\mathrm{D})} - \frac{kT}{6} \sum_i N_i \alpha_i^2 - \frac{2\pi}{27V} \sum_{i,j} N_i N_j m_i m_j \alpha_i \alpha_j - \frac{2\pi}{675V(kT)^2} \sum_{i,j} N_i N_j m_i^3 m_j^3 \alpha_i \alpha_j \sigma_{ij}^{-6} + O(H^3). \tag{17}$$

Assuming continuous polydispersity in dipole moment, the free energies can be expressed with the help of integrals containing the particle distribution functions [Eq. (5)]. The derived q2D magnetization functions that are proportional to the field derivatives of the corresponding free energies are

$$M_\parallel^{(\mathrm{q2D})} = \rho \overline{L(\alpha)} \left[1 + \frac{\pi}{2} \rho \overline{L'(\alpha)} \right], \tag{18}$$

and

$$M_\perp^{(\mathrm{q2D})} = \rho \overline{L(\alpha)} [1 - \pi \rho \overline{L'(\alpha)}], \tag{19}$$

where

$$\overline{L(\alpha)} = \int_0^\infty m(x) p(x) L[\alpha(x)] dx \tag{20}$$

and

$$\overline{L'(\alpha)} = \int_0^\infty m(x)p(x)L'[\alpha(x)]dx. \quad (21)$$

In these equations $L'(\alpha)$ is the field derivative of the Langevin function.

Equations (18) and (19) lead to the following susceptibilities:

$$\chi_{\parallel}^{(\mathrm{q2D})} = 4\pi\overline{\chi_L^{(\mathrm{q2D})}}\left[1 + \frac{11\pi}{6}\overline{\chi_L^{(\mathrm{q2D})}}\right], \quad (22)$$

and

$$\chi_{\perp}^{(\mathrm{q2D})} = 4\pi\overline{\chi_L^{(\mathrm{q2D})}}[1 - \pi\overline{\chi_L^{(\mathrm{q2D})}}], \quad (23)$$

where

$$\overline{\chi_L^{(\mathrm{q2D})}} = \frac{\rho}{3kT}\int_0^\infty m^2(x)p(x)dx, \quad (24)$$

which reduces, for the monodisperse system, to the Langevin susceptibility, $\chi_L = \rho m^2/(3kT)$. Here, it is assumed that the effective in-plane field strength is given by the Weiss mean-field approximation, $H_{\parallel\mathrm{eff}} = H_{\parallel} + (4\pi/3)M_{\parallel}$, but the out-of-plane component $H_{\perp\mathrm{eff}}$ is equal to $H_{\perp}$ due to the monolayer properties.

From Eq. (16) the initial susceptibility for 2D fluids reads

$$\chi^{(\mathrm{2D})} = 2\pi\overline{\chi_L^{(\mathrm{2D})}}[1 + \pi\overline{\chi_L^{(\mathrm{2D})}}], \quad (25)$$

where

$$\overline{\chi_L^{(\mathrm{2D})}} = \frac{\rho}{2kT}\int_0^\infty m^2(x)p(x)dx. \quad (26)$$

From Eq. (17) the initial susceptibility for 3D fluids can be written as

$$\chi^{(\mathrm{3D})} = 4\pi\overline{\chi_L^{(\mathrm{3D})}}\left[1 + \frac{4\pi}{3}\overline{\chi_L^{(\mathrm{3D})}}\left(1 + \frac{(\overline{m^2})^2}{25(kT)^2\bar{x}^6}\right)\right], \quad (27)$$

where $\overline{\chi_L^{(\mathrm{3D})}} = \overline{\chi_L^{(\mathrm{q2D})}}$. Considering the free energy expression [Eq. (17)], this equation is exact (in the framework of mean field approximation) for the monodisperse system (first obtained by Ivanov and Kuznetsova [22]), but it is only an approximation for the polydisperse one due to the last term containing the coefficient $(\overline{m^2})^2/\bar{x}^6$. [Without this approximation it is not possible to calculate analytically the last term of Eq. (17), because the $(2\sigma_{ij})^6 = (\sigma_i + \sigma_j)^6$ coupling hinders the factorization.] Eq. (27) can be considered as the improved version of the previous susceptibility formulas [21,12] of real polydisperse fluids.

C. Monte Carlo algorithm

Constant volume and temperature Monte Carlo calculations have been performed using translational-orientational and resizing moves of the particles (semigrand ensemble simulation). In our recent work [17] a simple scheme was constructed to produce appropriate distribution functions for the trial moves responsible for generating the possible configurations of particle sizes.

The original semigrand ensemble method [14] operates with a fixed underlying (sampling) particle distribution density $p_u(x)$ for the resizing moves. In our case, however, $p_u(x)$ is dynamically updated during the simulation in such a way as to minimize the deviation of the instantaneous particle distribution density $p_c(x)$ from the target distribution density $p(x)$. Starting from $p_u(x) = p(x)$ [or $p_u(x)$ is taken from the output of a previous run], at regular simulation intervals, the histogram approximation of $p_u(x)$ is adjusted for each entry of the distribution, x_i. Here, $p_c(x)$ is taken from a limited number of configurations immediately preceding the adjustment step. In our procedure, the adjustment ratio parameter (η) used to increase or decrease $p_u(x_i)$, if necessary, was kept fixed (5%) for each entry except for the low-probability particle size regions, where it was set proportional to the relative deviation of $p_c(x_i)$ from $p(x_i)$. In this work the adjustment ratio parameter is set proportional to the relative deviation in the whole range of particle sizes:

$$\eta_i = \gamma\left|\frac{p_c(x_i) - p(x_i)}{p(x_i)}\right|100 \quad (28)$$

for all x_i, where γ is the modification factor. Furthermore, the idea proposed by Wilding [20] is followed in the sense that a periodically decreasing modification factor is imposed. According to this procedure, a new simulation cycle starts when the maximum relative deviation of $\langle p_c(x_i)\rangle$ from $p(x_i)$ falls below a prescribed value (the brackets denote the ensemble average taken in the entire simulation cycle). In the beginning of the new cycle, γ is reduced by 50% and the accumulators for the particle distribution, thermodynamic and structural properties, etc. are reset.

Tuning $p_u(x)$ in this manner violates detailed balance. However, detailed balance is restored asymptotically as γ goes to zero, moreover, we can also take the final $p_u(x)$ as the input of a normal semigrand ensemble simulation in order to obtain the exact equilibrium results for the properties of interest [30].

D. Computational details

In all simulations $N = 500$ particles were employed. The last production cycle of the simulations varied between 300×10^6 and 500×10^6 trial moves. The frequency of attempting resizing moves was equal to that of the translational and orientational moves and, likewise, the acceptance criterion of the resizing moves was the same as that used for the translational and orientational moves [16].

The long-range dipolar interactions were treated using the Ewald summation with conducting boundary condition [31,32]: in this case the applied external field in 2D and 3D is identical to the internal field acting on particles throughout the simulation box. The formulas for the q2D and true 2D systems are taken from the works of Weis [4] and Gao *et al.* [7].

The results for the dipolar (magnetic) fluids are presented in reduced units, where the mean magnetic core diameter $\bar{x}$ is used for σ: $T^* = kT/\varepsilon$ is the reduced temperature, and $\rho^* = N\sigma^3/V$ or $\rho^* = N\sigma^2/V$ is the reduced density in 3D or 2D,

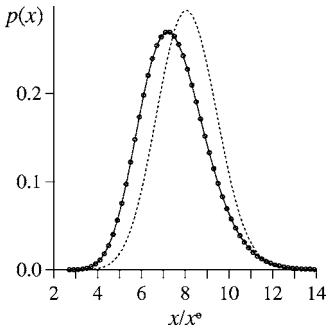

FIG. 1. The applied particle distribution density for the polydisperse systems: The continuous line indicates the target distribution. Data points show the average distribution obtained from a semigrand ensemble simulation in a q2D system at $T^*=1.0$, $\rho^*=0.60$, and $H_z^*=3.0$ (the field direction is perpendicular to the plane), and the dashed line is the underlying (sampling) distribution used here in the final simulation cycle.

where the volume V means the area of the plane in 2D and q2D. Furthermore, $H^*=H\sqrt{\sigma^3/\varepsilon}$ is the dimensionless external magnetic field, $M^*=M\sqrt{\sigma^3/\varepsilon}$ is the dimensionless magnetization, and $m^{*2}=m^2/(\varepsilon\sigma^3)$ is the reduced squared magnetic moment in q2D and 3D (in true 2D σ^3 is replaced by σ^2). For the magnetic coupling, $\lambda=m^{*2}/T^*=1$ was adopted at $T^*=1$. This choice implies that the average reduced magnetic moment was *unity* in all calculations.

The monodiperse fluid is characterized by uniform σ and m, with the additional specification that $m^*=1$. Due to the fact that $\bar{m}\propto\overline{x^3}$ (or $\bar{m}\propto\overline{x^2}$) and $\overline{x^3}\neq\bar{x}^3$ (or $\overline{x^2}\neq\bar{x}^2$) for the polydisperse fluid, the monodisperse fluid can be considered to have either a different mean core diameter or different bulk magnetization (i.e., different ferromagnetic component) than those of the polydisperse fluid. As the choice of σ is arbitrary to some degree, the equivalent monodisperse system might be the one with the same volume fraction of the magnetic cores as the polydisperse system (at the same number density). This means that, instead of the mean core diameter, the mean cubed core diameter would be identical for the two systems.

For the parameters of the gamma distribution, $x_0/x^\Theta=0.3$ and $a=24$ were taken, and the distribution was truncated at 2.6 and 14 nm, where $p(x)$ is already well below 4×10^{-4}. This truncation leads to a decrease of the original mean core diameter, $\bar{x}=x_0(a+1)=7.5$ nm, by only 0.04%. The distributions $p(x)$, $p_u(x)$, and $p_c(x)$ are stored in the form of a histogram with a prescribed number of subintervals or "bins." The width of the particle size subintervals was set to 0.2 nm. Figure 1 illustrates the good agreement between the target particle distribution and that obtained in the simulations.

III. RESULTS AND DISCUSSION

Magnetization curves were determined in q2D systems applying the external magnetic field parallel and perpendicular to the layer. We have compared the results for the polydisperse systems of different densities with those of the corresponding monodisperse systems. In the simulations the equilibrium magnetization can be obtained from the expression

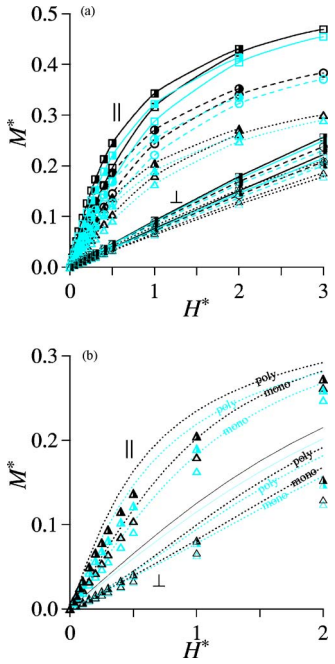

FIG. 2. (Color online) (a) Simulated dimensionless magnetization as a function of the external magnetic field in q2D systems obtained at $T^*=1.0$ (dark) and $T^*=1.1$ (light-colored), where ∥ and ⊥ stand for the direction of the external field (in-plane and out-of-plane, respectively). The triangles and the dotted lines correspond to ferrofluids at $\rho^*=0.40$, the circles and the dashed lines to ferrofluids at $\rho^*=0.50$, the squares and the solid lines to ferrofluids at $\rho^*=0.60$. Open and half-closed symbols denote the monodisperse and the polydisperse systems, respectively. The statistical uncertainties of the simulation results do not exceed the symbol size. (b) Comparison of the theoretical predictions (lines) with the simulation results (symbols) at $\rho^*=0.40$. The continuous lines represent the magnetization of the ideal ferrocolloid gas $[M_L^*=m^*\rho^*L(\alpha)]$.

$$\mathbf{M}^*=\frac{1}{V^*}\left\langle\sum_{i=1}^{N}\mathbf{m}_i^*\right\rangle, \tag{29}$$

where the brackets denote the ensemble average. In our case, essentially zero net magnetizations were detected in the directions perpendicular to the applied field direction. Figure 2(a) shows that the density dependence and the temperature dependence of the results are consequential: the magnetization data are smaller at lower densities and higher temperatures. The smaller out-of-plane magnetizations reflect the preferred in-plane orientations of the dipole vectors. As we experienced, the linear relationship between M^* and H^* for these curves will break down only at strong magnetic fields, while the in-plane magnetization saturates more rapidly. This figure also reveals that both the in-plane and the out-of-plane magnetizations are greater in the polydisperse system than in its monodisperse counterpart. Figure 2(b) illustrates the quality of the theoretical prediction. The agreement between simulation and theory is better at weak external fields. At

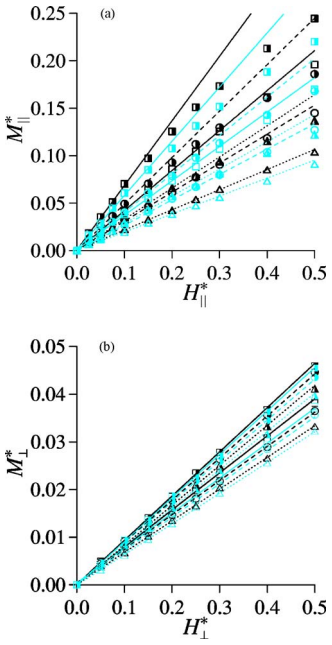

FIG. 3. (Color online) Dimensionless in-plane (a) and out-of-plane (b) magnetizations as a function of the external magnetic field in q2D systems obtained at $T^*=1.0$ (dark) and $T^*=1.1$ (light-colored). The meaning of the lines and symbols is the same as in Fig. 2. The straight lines are the linear fitting results, the slope of which gives the initial susceptibility.

stronger fields, the applied theory only yields the expected greater magnetization for the polydisperse system as compared to the monodisperse one and correctly predicts the temperature dependence of this property.

The initial gradient of the magnetization curve is the initial susceptibility χ, which is determined from the linear magnetic response $\mathbf{M}=(\chi/4\pi)\mathbf{H}$ at field strength $H\to 0$. To evaluate these data from simulation we need to ascertain the linear region of each simulated magnetization curve. Figure 3 shows the best linear fits to the initial regions of the in-plane and out-of-plane curves. Since there is no spontaneous magnetization in our case, the starting point of these fits was the origin, although we have taken into account the statistical errors of the simulation results for the other points. In general, χ can also be obtained from zero field simulations through fluctuation formulas. In 3D this reads

$$\chi^{(3D)}=\frac{4\pi V^*}{3T^*}(\langle \mathbf{M}^{*2}\rangle-\langle \mathbf{M}^*\rangle^2). \tag{30}$$

Similarly, the in-plane susceptibility in q2D can be calculated from

$$\chi_{\parallel}^{(q2D)}=\frac{4\pi V^*}{2T^*}(\langle \mathbf{M}_{\parallel}^{*2}\rangle-\langle \mathbf{M}_{\parallel}^*\rangle^2), \tag{31}$$

where the isotropy in 2D plane is considered through division by 2. Retaining the formal definition for χ, the out-of-plane susceptibility should be proportional to the fluctuation of the z component of $\mathbf{M}$ (the axial direction z is perpendicular to the layer, $M^*_{\perp}=M^*_z$):

$$\chi_{\perp}^{(q2D)}=\frac{4\pi V^*}{T^*}(\langle M_z^{*2}\rangle-\langle M_z^*\rangle^2). \tag{32}$$

We have found excellent agreement between the results for the susceptibility calculated from the explicit magnetic response of the system to the external field and from the zero field fluctuation formulas. These cross-checked simulation results are compiled in Table I. Here it is also seen that the efficiency of this simple first order perturbation theory in q2D is quite good for the in-plane susceptibility though the theory slightly overestimates the simulation results. However, this theory with the used order of truncation cannot adequately predict the density and temperature dependences of the out-of-plane susceptibilities.

In order to compare the above results with true 2D and 3D susceptibilities, we have defined a hypothetical "isotropic" susceptibility utilizing the system symmetry in q2D:

$$\chi^{(q2D)}=(2\chi_{\parallel}^{(q2D)}+\chi_{\perp}^{(q2D)})/3. \tag{33}$$

The true 2D and 3D susceptibilities were calculated from zero field simulations. The fluctuation formula in true 2D can be written as

$$\chi^{(2D)}=\frac{2\pi V^*}{2T^*}(\langle \mathbf{M}^{*2}\rangle-\langle \mathbf{M}^*\rangle^2). \tag{34}$$

Figure 4 shows the comparison between the results obtained from simulation and theory in systems of different dimensions. Since ordering in any system basically arises due to a competition between the particle interaction energy and the thermal energy, the susceptibility data are plotted here in

TABLE I. Magnetic susceptibility (χ) for the monodisperse and polydisperse ferrofluids in q2D systems obtained from simulation and theory.

		Monodisperse				Polydisperse			
T^*	ρ^*	$\chi_{\parallel}^{\text{sim.}}$	$\chi_{\parallel}^{\text{theory}}$	$\chi_{\perp}^{\text{sim.}}$	$\chi_{\perp}^{\text{theory}}$	$\chi_{\parallel}^{\text{sim.}}$	$\chi_{\parallel}^{\text{theory}}$	$\chi_{\perp}^{\text{sim.}}$	$\chi_{\perp}^{\text{theory}}$
1.0	0.4	2.7	3.0	0.80	0.97	4.2	4.8	1.03	0.97
1.0	0.5	3.8	4.1	0.90	1.00	6.2	6.7	1.13	0.80
1.0	0.6	5.4	5.4	0.97	0.93	8.4	9.0	1.16	0.46
1.1	0.4	2.3	2.6	0.78	0.94	3.6	4.1	1.01	1.00
1.1	0.5	3.3	3.6	0.88	1.00	5.2	5.8	1.08	0.90
1.1	0.6	4.5	4.7	0.93	0.98	7.2	7.7	1.12	0.66

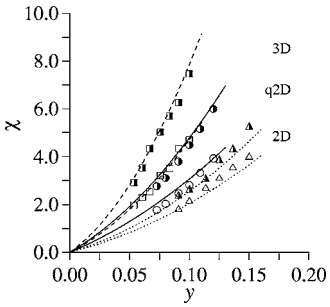

FIG. 4. Initial susceptibilities for 2D (triangles and dotted lines), q2D (circles and solid lines), and 3D (squares and dashed lines) systems as a function of the dimensionless parameter y. Symbols represent the simulation results and lines are the theoretical predictions. Open and half-closed symbols denote the monodisperse and the polydisperse systems, respectively. Note that these results are obtained from calculations at two different temperatures.

terms of the dimensionless parameter $y=\rho^*\lambda/\theta$. This parameter is a measure for the approximate zero field magnetic interaction energy of the system, $N^2/2m^{*2}/V^*$, relative to the thermal energy, $(N/2)\theta T^*$, where θ is the translational and rotational degrees of freedom of the particles (θ=4, 5, and 6 in 2D, q2D, and 3D, respectively). Note that the magnetic moments of the particles in true 2D were taken proportional to the area of the 2D disks. The obtained susceptibility curves shift consistently downward as the system dimensionality and thus the degrees of freedom of particle motions decreases. Also, the consistent influence of polydispersity is clearly seen. The applied theory predicts the susceptibilities in all dimensions with good to excellent accuracy, which verifies the efficiency of this simple theory also for q2D systems.

The pair correlation functions, $g(r)$, determined from simulations in systems of different dimensions for the same y are presented in Fig. 5. As expected, notable broadening and shifting of peaks can be observed for the polydisperse systems as compared to the monodisperse ones. However, for both the monodisperse and the polydisperse cases, the deviations between the curves reflect only the density differences between the 2D, q2D, and 3D systems considered here (we get practically indistinguishable pair correlation functions for

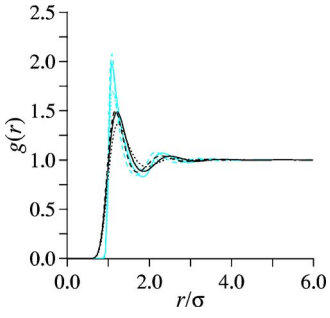

FIG. 5. (Color online) Pair correlation functions for 2D systems at $\rho^*=0.40$ (dotted lines), q2D systems at $\rho^*=0.50$ (solid lines), and 3D systems at $\rho^*=0.60$ (dashed lines) in the absence of the external field at $T^*=1.0$. Light-colored and dark curves denote the monodisperse and the polydisperse systems, respectively.

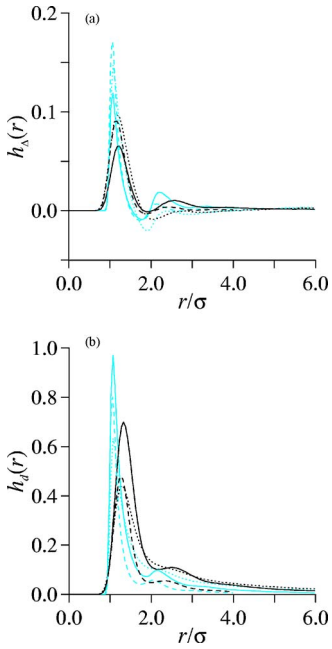

FIG. 6. (Color online) Projections of the pair correlation functions. The meaning of the lines is the same as in Fig. 5.

2D and q2D systems at the same density). The correlation functions $h_\Delta(r)$ and $h_d(r)$ provide a deeper insight into the structure. These functions are the projections of $g(r)$ onto the functions

$$\Delta(i,j)=\frac{\mathbf{m}_i}{m_i}\cdot\frac{\mathbf{m}_j}{m_j} \tag{35}$$

and

$$d(i,j)=3\left(\mathbf{m}_i\cdot\frac{\mathbf{r}_{ij}}{r_{ij}}\right)\left(\mathbf{m}_j\cdot\frac{\mathbf{r}_{ij}}{r_{ij}}\right)-\mathbf{m}_i\cdot\mathbf{m}_j \tag{36}$$

(in true 2D factor 3 is replaced by 2). $h_\Delta(r)$ and $h_d(r)$ are measures of the relative orientation of a pair of dipoles and their dipolar interaction energy at a given separation, respectively. Figure 6 indicates that the first peak in $h_\Delta(r)$ and $h_d(r)$ in the polydisperse systems tends to be rounded rather than sharp as in the monodisperse systems. The more pronounced shift of this peak in $h_d(r)$ obviously comes from the significant contribution of the pairs of larger dipoles to the average attractive interaction at short separation distances [note that $d(i,j)$ is defined here by taking into account the lengths of the dipole vectors]. The fact that the first minimum in $h_\Delta(r)$ is the deepest for the true 2D system demonstrates that the second neighbors have particularly limited opportunities to find favorable orientations in 2D. Of the three systems, the q2D system exhibits the weakest orientational ordering but the strongest attraction of dipoles in the first shell. This suggests that, in the absence of the external field, the dipole moments in q2D point preferably in the plane, since there is a higher probability for a given number of particle pairs with nearly parallel dipole moments in a 2D shell, in contrast to a 3D shell, to be found in nearly colinear arrangement with the interparticle separator vector. Furthermore, although the

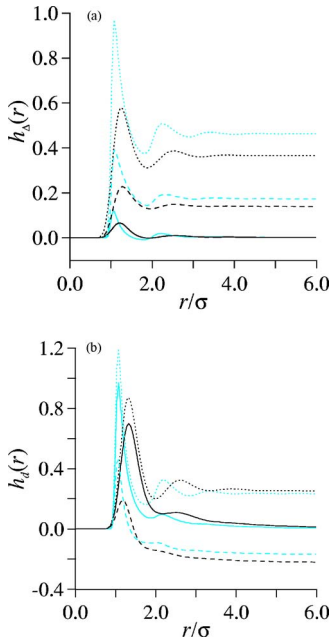

FIG. 7. (Color online) Projections of the pair correlation functions in q2D systems at $T^*=1.0$ and $\rho^*=0.50$. The solid lines represent the zero field results, the dashed and the dotted lines stand for the results obtained at $H_z^*=3.0$ (the field direction is perpendicular to the plane) and at $H_x^*=2.0$ (the field direction is parallel to the plane), respectively. Light-colored and dark curves denote the monodisperse and the polydisperse systems, respectively.

alignment of dipoles in the plane is better in 2D than in q2D, the short-range attraction of 3D dipolar bodies is stronger than that of 2D dipolar disks.

Figure 7 shows the effect of the external field on the shape of these correlation functions in q2D. The results for $h_\Delta(r)$ are consistent with the magnetization curves in that the orientational ordering is significantly weaker when applying the external field perpendicular to the layer. The systematic decrease in angular correlation due to polydispersity suggests a substantially lower ability of the smaller particles to coalign with the field direction. Consequently, when considering the observed greater magnetization of the polydisperse system, $h_\Delta(r)$ indirectly uncovers the decisive role of the larger particles in the magnetic properties of the polydisperse system. The negative values in $h_d(r)$ make evident the net repulsion between the dipoles induced by the external field pointing along the z axis. For the case of perpendicular fields, we have found the total potential energy consistently lower (and negative) in the polydisperse systems than in the monodisperse ones (the numerical results are not presented here). In light of this, the most striking observation here is that the polydisperse system exhibits greater net repulsion between the dipoles. Since the average magnetic moment is the same for all systems studied, this can only be attributed to the fact that the large dipoles align predominantly in the field direction, and the energy gain from the interactions of these particles with the external field not only compensates the comparatively small contribution of the smaller particles to the external part of the potential energy but also the greater net repulsion between the particles.

IV. CONCLUSIONS

We considered the effect of polydispersity on the magnetic properties of model ferrofluid monolayers with a medium degree of fixed polydispersity. On the basis of the first order high field approximation perturbation theory, the magnetization curves in q2D and the Langevin susceptibility dependence of the initial magnetic susceptibility in 2D, 3D, and q2D are predicted. The obtained equilibrium magnetization curves and dipolar correlation functions reflect the dissimilarity in composition and thus in structure between the polydisperse systems and their monodisperse counterparts. The calculations provide further evidence of the preferred in-plane orientation of the magnetic dipoles and of the crucial role of the large dipoles in the magnetic properties of the polydisperse q2D systems. In comparison with the true 2D and 3D systems, the initial magnetic susceptibility was found to be remarkably sensitive to the degrees of freedom of particle motions.

ACKNOWLEDGMENTS

The authors give due thanks to the National Information Infrastructure Development Office (NIIF) for providing computing time on their supercomputer. Financial support from the Hungarian Scientific Research Fund (Grant No. OTKA-TO38239) is acknowledged.

[1] A. Satoh, R. W. Chantrell, S.-I. Kamiyama, and G. N. Coverdale, J. Colloid Interface Sci. **178**, 620 (1996).
[2] E. Lomba, F. Lado, and J. J. Weis, Phys. Rev. E **61**, 3838 (2000).
[3] J. M. Tavares, J. J. Weis, and M. M. Telo da Gama, Phys. Rev. E **65**, 061201 (2002).
[4] J. J. Weis, J. Phys.: Condens. Matter **15**, S1471 (2003).
[5] P. D. Duncan and P. J. Camp, J. Chem. Phys. **121**, 11322 (2004).
[6] J. J. Weis, Mol. Phys. **103**, 7 (2005).
[7] G. T. Gao, X. C. Zeng, and W. Wang, J. Chem. Phys. **106**, 3311 (1997).
[8] R. E. Rosensweig, *Ferrohydrodynamics* (Cambridge University Press, Cambridge, 1985).
[9] B. Huke and M. Lücke, Rep. Prog. Phys. **67**, 1734 (2004).
[10] A. O. Ivanov, J. Magn. Magn. Mater. **201**, 234 (1999).
[11] T. Kristóf, J. Liszi, and I. Szalai, Phys. Rev. E **69**, 062106 (2004).
[12] T. Kristóf and I. Szalai, Phys. Rev. E **68**, 041109 (2003).
[13] M. Aoshima and A. Satoh, J. Colloid Interface Sci. **288**, 475 (2005).
[14] M. R. Stapleton, D. J. Tildesley, and N. Quirke, J. Chem. Phys. **92**, 4456 (1990).
[15] T. Kristóf and J. Liszi, Mol. Phys. **99**, 167 (2001).

[16] D. A. Kofke and E. D. Glandt, J. Chem. Phys. **87**, 4881 (1987).
[17] T. Kristóf, J. Liszi, and I. Szalai, Phys. Rev. E **71**, 031109 (2005).
[18] N. B. Wilding and P. Sollich, J. Chem. Phys. **116**, 7116 (2002).
[19] F. A. Escobedo, J. Chem. Phys. **115**, 5642 (2001).
[20] N. B. Wilding, J. Chem. Phys. **119**, 12163 (2003).
[21] Yu. A. Buyevich and A. O. Ivanov, Physica A **190**, 276 (1992).
[22] A. O. Ivanov and O. B. Kuznetsova, Phys. Rev. E **64**, 041405 (2001).
[23] S. W. deLeeuw, J. W. Perram, and E. R. Smith, Annu. Rev. Phys. Chem. **37**, 245 (1986).
[24] A. Tani, D. Henderson, J. A. Barker, and C. E. Hecht, Mol. Phys. **48**, 863 (1983).
[25] M. Valiskó and D. Boda, J. Phys. Chem. B **109**, 6355 (2005).
[26] Z. Wang, C. Holm, and H. W. Müller, Phys. Rev. E **66**, 021405 (2002).
[27] C. G. Joslin, Mol. Phys. **49**, 129 (1983).
[28] M. I. Shliomis, A. F. Pshenichnikov, K. I. Morozov, and I. Yu. Shurubor, J. Magn. Magn. Mater. **85**, 40 (1990).
[29] T. Kristóf and I. Szalai, J. Magn. Magn. Mater. (to be published).
[30] While completing this manuscript we discovered the appearance of a new work: D. Frydel and S. A. Rice, Phys. Rev. E **71**, 041403 (2005). The authors suggest a very similar scheme for handling fixed polydispersities in simulations with constant overall number density.
[31] S. W. de Leeuw, J. W. Perram, and E. R. Smith, Proc. R. Soc. London, Ser. A **373**, 27 (1980).
[32] M. P. Allen and D. J. Tildesley, *Computer Simulation of Liquids* (Clarendon Press, Oxford, 1987).